Letter

Ferroelectric structural transition in hafnium oxide induced by charged oxygen vacancies

Ri He,[1,*] Hongyu Wu,[1,*] Shi Liu,[2] Houfang Liu,[3] and Zhicheng Zhong[1,4,†]

[1]*Key Laboratory of Magnetic Materials Devices & Zhejiang Province Key Laboratory of Magnetic Materials and Application Technology, Ningbo Institute of Materials Technology and Engineering, Chinese Academy of Sciences, Ningbo 315201, China*

[2]*School of Science, Westlake University, Hangzhou, Zhejiang 310024, China; Institute of Natural Sciences, Westlake Institute for Advanced Study, Hangzhou, Zhejiang 310024, China; and Key Laboratory for Quantum Materials of Zhejiang Province, Hangzhou Zhejiang 310024, China*

[3]*Institute of Microelectronics and Beijing National Research Center for Information Science and Technology (BNRist), Tsinghua University, Beijing 100084, China*

[4]*China Center of Materials Science and Optoelectronics Engineering, University of Chinese Academy of Sciences, Beijing 100049, China*

(Received 26 March 2021; revised 11 November 2021; accepted 12 November 2021; published 29 November 2021)

The discovery of ferroelectric HfO_2 in thin films and more recently in bulk is an important breakthrough because of its silicon compatibility and unexpectedly persistent polarization at low dimensions, but the origin of its ferroelectricity is still under debate. The stabilization of the metastable polar orthorhombic phase was often considered as the cumulative result of various extrinsic factors such as stress, grain boundary, and oxygen vacancies as well as phase transition kinetics during the annealing process. We propose a mechanism to stabilize the polar orthorhombic phase over the nonpolar monoclinic phase that is the bulk ground state. Our first-principles calculations demonstrate that the doubly positively charged oxygen vacancy, an overlooked defect but commonly presenting in binary oxides, is critical for the stabilization of the ferroelectric phase. The charge state of the oxygen vacancy serves as a degree of freedom to control the thermodynamic stability of competing phases of wide band gap oxides.

DOI: 10.1103/PhysRevB.104.L180102

The discovery of unusual ferroelectricity in fluorite-structural hafnium oxide (HfO_2) has attracted considerable attention because of its silicon compatibility and unexpectedly robust ferroelectricity at low dimensions compared to conventional perovskite-based ferroelectrics [1–7]. However, there is still an important, unresolved issue regarding the origin of ferroelectricity, that is, the stability puzzle: The polar orthorhombic (PO) $Pca2_1$ phase is ferroelectric but metastable [8–10], while the nonpolar monoclinic (M) phase is the ground state [11], and both phases often coexist in ferroelectric HfO_2-based thin films [12,13]. Previous experimental and theoretical works have put their efforts into identifying the mechanism(s) to stabilize the PO phase, which can be roughly classified into thermodynamic models (including various extrinsic factors such as doping, grain size effect, strain, and electric field) and kinetic models (accounting for phase transition barriers during the annealing process) [7,10–12,14–22]. However, a simple strategy to stabilize the PO phase remains elusive. Among the proposed mechanisms, the oxygen vacancy is brought into sharp focus for the following reasons. First, oxygen vacancy is a dominant intrinsic defect in HfO_2 thin films which is unavoidable and often found at a relatively high concentration of 1.7×10^{21} cm^{-3} (corresponding to HfO_{2-x} with $x = \sim 2.65\%$) in experiments [23,24]. Second, there have been experimental observations that the M phase transforms to the PO phase when oxygen vacancies migrate from the interface into the bulk region [23,25], and high oxygen vacancy concentration can suppress the M phase and stabilize the PO phase [26]. A very recent experimental work reported that ferroelectricity in HfO_2-based film is intertwined oxygen vacancy migration, and oxygen vacancy migration can induce structural phase transitions [27]. Nevertheless, they claimed that the nature of the coupling between the oxygen vacancy and ferroelectricity "remains agnostic." Theoretical studies have reported that the energy difference between the PO phase and the M phase will slightly decrease as the concentration of the charge neutral oxygen vacancy (V_O) increases; however, even at an extremely high concentration of ~12%, the energy of the PO phase is still substantially higher than that of the M phase [5,14,15,28]. It is evident that the oxygen vacancy alone cannot solve the stability puzzle. Moreover, first-principles calculations also indicate that the diffusion barrier of V_O in HfO_2 is too high (~3 eV) to be mobile [29,30], which also conflicts with the experimental observations [23,31].

These experiment-theory conundrums regarding oxygen vacancies in HfO_2 may derive from an additional degree of freedom: the defect charge state. The charge states of a defect iare a subject that has been widely studied in semiconductors; previous theoretical works focus on their formation energies, transition levels, etc. [32,33]. In particular, oxygen vacancies are known to possess different charge states such as the doubly positively charged state (V_O^{2+}) in various oxides including HfO_2 [34,35]. To our best knowledge, few theoretical studies of the effect of V_O^{2+} on the phase stability of oxides have been

*These autors contributed equally to this work.
†zhong@nimte.ac.cn

performed on HfO_2, though a similar idea has been performed in ZrO_2 using the self-consistent tight-binding model [36]. Using density functional theory (DFT) calculations, we find that a V_O^{2+} concentration of 2.35% is enough to make the PO phase thermodynamically more stable than the M phase in HfO_2. More important, we thoroughly study the effect of V_O^{2+} on the relative phase stability in various wide band gap oxides. We propose that for wide band gap oxides, by comparing the absolute energy of defect levels induced by charge neutral V_O in different competing phases, the relative thermodynamic stability between competing phases containing charged oxygen vacancies can be determined. Furthermore, we find that V_O^{2+} exhibits lower diffusion barriers than that of V_O in HfO_2, indicating the mobile oxygen vacancy observed in experiments is likely at the +2 charge state. These results provide insight into the origin of ferroelectricity of HfO_2 and may help to explain the vacancy-induced structural phase transition in HfO_2.

The DFT calculations show that the lattice relaxation around V_O is negligibly weak, while being remarkably strong around V_O^{2+} in the M phase. For V_O (removing a fourfold coordinated oxygen atom), the four neighboring Hf atoms are displaced outward by ∼0.013 Å and neighboring O atoms are displaced inward by ∼0.035 Å from their original lattice positions, corresponding to 0.6% and 1.6% of the equilibrium Hf-O bond length, respectively. For charged defects, the artificial compensating jellium background charge was used (for details, see Methods section in Supplemental Material [37]). In the case of V_O^{2+}, the neighboring Hf atoms have outward displacements of ∼0.18 Å, and the surrounding O atoms are distorted inward by ∼0.23 Å, as shown by blue and green arrows in Fig. 1(a). The atomic displacements induced by V_O^{2+} are about 8.6%–11.0% of the equilibrium Hf-O bond length, nearly ten times the values around the charge neutral V_O. The displacements decay exponentially with increasing distance from the vacancy site (see Supplemental Material, Fig. S1 [37]; also see Refs. [38–47]). A similar effect of oxygen vacancy on lattice relaxations is also found in the PO phase in which the local atomic distortions around V_O^{2+} are much larger than those around V_O.

The markedly different lattice relaxations around V_O and V_O^{2+} result from the distinctions of their electronic structures. The removal of an oxygen atom leads to a doubly occupied defect state within the band gap [see Fig. 1(b)] due to the wide band gap of HfO_2, while in narrow band gap oxides such as $SrTiO_3$, the defect states will merge with the bottom of the empty conduction band states, making the system metallic [48]. It is well known that semilocal density functionals such as Perdew-Burke-Ernzerhof (PBE) will underestimate the band gap. Considering that the PBE band gap of HfO_2 from our DFT calculations is already quite large (∼4 eV), a further enhancement of the band gap (i.e., predicted with hybrid functionals such as HSE06) will only increase the tendency of electron localization around the vacancy site and the formation of a doubly occupied defect state within the band gap. Therefore, the presence of in-gap defect states is robust for wide band gap oxides [49] (we also perform calculations using the HSE functional; see Supplemental Material, Fig. S5 [37]). It is also worth noting that in Fig. 1(b), we plot the density of states (DOS) with respect to the absolute energy

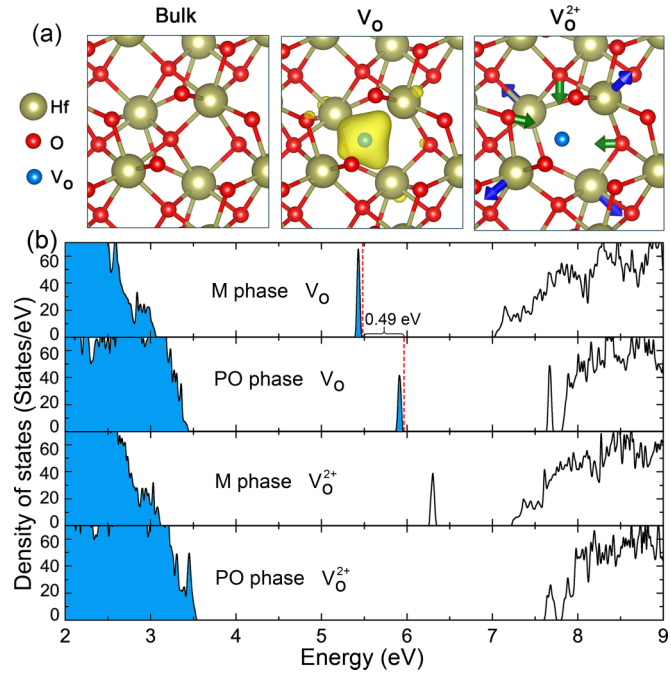

FIG. 1. (a) Defect-free atomic structure of M-phase HfO_2 and the local atomic relaxations around the V_O and V_O^{2+}; yellow surface represents the charge density isosurface of the doubly occupied defect state due to V_O; the strong outward and inward displacements of neighboring Hf and O atoms around V_O^{2+} are indicated by blue and green arrows. (b) Density of states of different phases of HfO_2 with V_O and V_O^{2+}; blue shaded areas represent occupied states. The values of doubly occupied defect levels are shown by red dashed lines. The energy difference of defect levels ($\Delta\varepsilon_D$) is 0.49 eV.

instead of setting the Fermi level to zero as usual because the bulk systems of PO and M phases have a common energy reference at the same charge state; thus we mark the energy difference of 0.49 eV between the defect levels in the M and PO phases, which will be a focal point in our later discussions. The two excess electrons occupying the in-gap defect states are strongly localized at the oxygen vacancy site, as shown in Fig. 1(a). This unusual electronic structure is similar to the electride materials filled with localized electrons in crystal voids [50]. The two localized electrons act effectively as an O^{2-} in the perfect crystal of HfO_2; therefore the neighboring atoms around V_O can barely sense the removal of an oxygen atom and remain nearly undistorted. Conversely for V_O^{2+}, the neighboring atoms can sense the vacancy and the balance of the lattice structure is broken, thus leading to strong lattice relaxations.

To investigate the influence of the charge state of oxygen vacancies on phase stability, we defined ΔE as the energy difference between the PO and M phases as a function of the concentration of oxygen vacancies: $\Delta E(C^n_{V_O}) = E_{PO}(C^n_{V_O}) - E_M(C^n_{V_O})$, where C_{V_O} represents the concentration of oxygen vacancies, superscript n represents the charge state of the vacancy, and $n = 0$ and $+2$ are used in calculations. In a $2 \times 3 \times 2$ supercell with 96 O atoms, removing one oxygen atom corresponds to HfO_{2-x} with $x = 2.08\%$. The PO and M phases are modeled with supercells of the same size containing the same number of atoms. This allows a direct

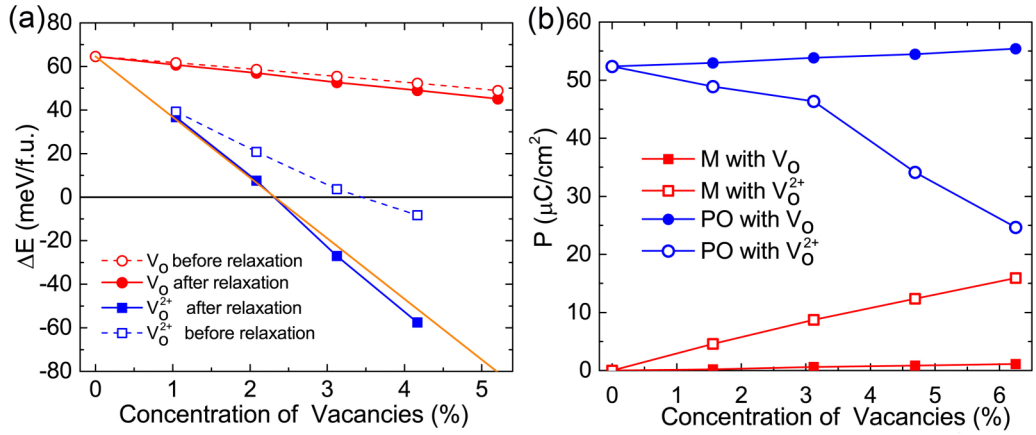

FIG. 2. (a) Energies of the PO phase of HfO_2 with different vacancy charge states and relaxation conditions relative to the M phase (ΔE) as a function of vacancy concentration obtained with $2 \times 3 \times 2$ supercells. (b) Vacancy concentration dependence of local polarization for PO and M phases with oxygen vacancy at different charge states.

comparison of the absolute energies between the PO and M phases at the same charge state. A negative value of ΔE indicates the PO phase is energetically more favorable than the M phase.

The calculation results show that V_O in HfO_2 cannot stabilize the ferroelectric PO phase, because ΔE only slightly reduces but remains positive with the increasing concentration of V_O as illustrated in Fig. 2(a), which agrees well with previous theoretical studies [5,15,28]. For V_O^{2+}, as illustrated in Fig. 2(a), ΔE decreases gradually from 36.7 to -57.5 meV/f.u., as the concentration of V_O^{2+} increases from 1.04% to 4.16% (corresponding to one and four vacancies in the supercells). This indicates that V_O^{2+} can stabilize the PO phase more effectively than V_O and it is in good agreement with experimental observation that high oxygen vacancy concentration can suppress the M phase and stabilize the PO phase [26]. We observe a linear relationship between the concentration of V_O^{2+} and ΔE [yellow line in Fig. 2(a)] at low concentrations ($C_{V_O^{2+}} < 2.0\%$); the extrapolation gives a critical concentration of 2.35% above which the PO phase is more stable thermodynamically than the M phase. This value agrees well with results from direct DFT calculations for high concentrations which are shown by the blue solid squares in Fig. 2(a). We consider that the artificial compensating background charge in the supercell contributes to electrostatic energy and such contribution may be different in the M and PO phase. Therefore, it is necessary to exclude the influence of the compensating background charge to the reduction of ΔE. In order to study the V_O^{2+} and avoid introducing an artificial compensating background charge, we constructed the supercells with complex defects by removing an O atom and substituting Sr (2+ valence state) for Hf (4+ valence state) as shown in Fig. S7 in the Supplemental Material [37]. The complex defects calculation results show that the effective V_O^{2+} ($Sr_{Hf} + V_O$) could reduce the similar magnitudes of energy difference between PO and M phase compared to V_O^{2+} (see Table S1 [37]). It proves that the charge vacancy induced stabilization effect is not dependent on the assumption of an artificial compensating background charge in the calculations. In addition, we change the volume of the supercells with V_O^{2+}, and found that the ΔE's of different volume systems have similar values (see Table S2 [37]). It is also found that the V_O^{2+}-induced stabilization effect is presented even without atomic relaxations [see blue dashed line in Fig. 2(a)]. Therefore, it can be concluded that the volume change and ion relaxation are not the dominant factors responsible for the drastic reduction of ΔE. The reduction of ΔE mainly originates from the reduction of the electrostatic energy due to the removal of two localized electrons at the oxygen vacancy site, as discussed in detail below. A similar trend is found for threefold coordinated charged oxygen vacancies in other phases of HfO_2 (see Supplemental Material, Figs. S2 and S3 [37]). The nonpolar orthorhombic *Pbca* phase (AO) is another possible candidate for the ground state configuration in HfO_2. We also investigate the effect of V_O^{2+} on the competition between the AO and PO phases. As revealed in Figs. S2 and S3 [37], the V_O^{2+} tends to stabilize both the AO and PO over the M phase, while the energy of the nonpolar AO phase remains lower by about 20 meV/f.u. than the polar PO phase at low V_O^{2+} concentrations (<2%). The calculations also reveal that when the V_O^{2+} concentration is relatively high (>4%), the PO and AO phases have very similar energy, indicating that the two phases may coexist in HfO_2 ferroelectric films.

In addition to the ferroelectric phase stability, the magnitude of polarization is rather crucial for device applications. We find V_O^{2+} only slightly weakens the magnitude of the polarization of the PO phase. In comparison, V_O enhances the polarization. As shown in Fig. 2(b), the polarization magnitude decreases with the increasing V_O^{2+} concentration in the PO phase. For instance, ~3% of V_O^{2+} will reduce the polarization from 52.2 to 46.7 $\mu C/cm^2$, but the resultant polarization magnitude remains within the acceptable range of electronic devices application. The suppressed polarization induced by charged oxygen vacancies might be one of the reasons why the experimental polarization value is usually lower than the ideal magnitude of 52.2 $\mu C/cm^2$ from first-principles calculation [1,4,7,23,25].

Considering that oxygen vacancy is common in oxides, we systematically examined the relationship between V_O^{2+} and phase stability in a few representative oxides, and identify a

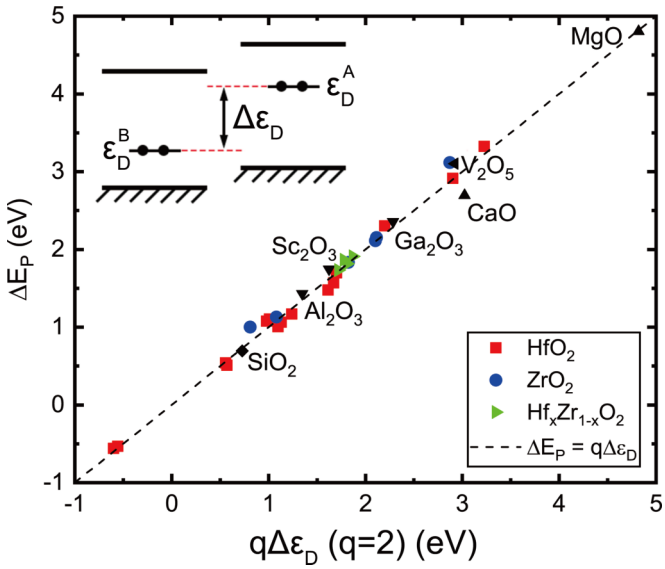

FIG. 3. The energy differences of defect levels multiplied by the effective charge ($q\Delta\varepsilon_D$) versus relative phase stability [ΔE_P in Eq. (4)] in various wide band gap oxides.

general trend. We propose a thermodynamic cycle connecting the energy difference between two competing phases (phase A and B with B lower in energy) and the in-gap defect level energy difference [$\Delta\varepsilon_D$ in Eq. (1)].

$$\Delta\varepsilon_D = \varepsilon_D^A - \varepsilon_D^B, \tag{1}$$

$$E^A(\mathrm{V_O}) = E^A\left(\mathrm{V_O^{2+}}\right) + q\varepsilon_D^A, \tag{2}$$

$$E^B(\mathrm{V_O}) = E^B\left(\mathrm{V_O^{2+}}\right) + q\varepsilon_D^B. \tag{3}$$

It is noted that ε_D is the energy of the defect level due to $\mathrm{V_O}$; superscripts indicate that they correspond to phases A and B, as illustrated in the inset of Fig. 3. $E(\mathrm{V_O})$ and $E(\mathrm{V_O^{2+}})$ in Eqs. (2) and (3) indicate the total energy of the specific phase with $\mathrm{V_O}$ or $\mathrm{V_O^{2+}}$ by DFT calculation, respectively. We then define ΔE_P, and subtract Eq. (2) from Eq. (3) to get Eq. (4). Equation (4) is the relative phase stability in the presence of $\mathrm{V_O}$ and $\mathrm{V_O^{2+}}$, respectively.

$$\begin{aligned}\Delta E_P &= [E^A(\mathrm{V_O}) - E^B(\mathrm{V_O})] - \left[E^A\left(\mathrm{V_O^{2+}}\right) - E^B\left(\mathrm{V_O^{2+}}\right)\right] \\ &= q\Delta\varepsilon_D.\end{aligned} \tag{4}$$

Therefore, ΔE_P reflects the change in relative phase stability when the charge state of oxygen vacancy becomes 0 to +2. The key assumption in the thermodynamic cycle is that for wide band gap oxides, the energy of localized charge q at a vacancy is simply $q\varepsilon_D$, and thus ΔE_P is equal to $q\Delta\varepsilon_D$ ($q = 2$). A positive value of ΔE_P means the presence of $\mathrm{V_O^{2+}}$ has the tendence to stabilize the A phase relative to the B phase, potentially driving a phase transition from B to A. It is evident that $\mathrm{V_O^{2+}}$ will reduce more energy of the A phase if $\varepsilon_D^A > \varepsilon_D^B$. Take the PO phase and the M phase in HfO_2 as an example; the energy of removing two excess electrons in the PO phase is 1.08 eV higher than that in the M phase. This value is approximately equal to twice the difference between defect levels (0.49 eV) which we marked in Fig. 1(b). As we discussed above, in wide band gap oxides, the effective charge from $\mathrm{V_O}$ is strongly localized at the vacancy site and does not bond with atoms around the defect. Therefore, the energy of the defect level is mainly contributed by the Hartree potential of the surrounding atoms, and the Hartree potential can be well described by DFT calculations. Due to the different arrangement of atoms around the defect in different phases, their Hartree potentials are also different, which is reflected in the difference of defect levels ($\Delta\varepsilon_D$). That is why for the PO phase and the M phase in HfO_2, ΔE_P is approximately equal to $q\Delta\varepsilon_D$.

The above conclusion about the relationship between ΔE_P and $q\Delta\varepsilon_D$ should be general for wide band gap oxides, and even for ionic insulators. Because the Hartree potential and electrostatic energy is universal, and the important factor here is a large band gap that can form a localized defect level, the elemental composition and crystal structure of the material are less irrelevant. We first focus on hafnium dioxide and zirconium dioxide (ZrO_2), checking the ΔE_P of their various phases relative to the M phase. As shown in Fig. 3, the coordinate of each dot is ($q\Delta\varepsilon_D$, ΔE_P) and all dots are located around the dashed line which represents $q\Delta\varepsilon_D = \Delta E_P$. We also calculate the oxygen vacancy in oxides of various valence states, of which the band gap obtained by PBE is larger than 3.5 eV, as shown in Fig. 3 (see Table S5 in the Supplemental Material for detailed data [37]); they are also located around the dashed line. Figure 3 indicates that $q\Delta\varepsilon_D = \Delta E_p$ is a universal phenomenon in wide band gap oxides. It means that for two specific phases of certain wide band gap oxides, the $\mathrm{V_O^{2+}}$ will significantly reduce the total energy of one phase relative to the other phase, and induce a phase transition. We notice that previous works focus on researching the formation energy of different charged defects in one certain system. The important parameter there is the chemical potential for the effective charge and atoms being removed or added [51–53]. The chemical potential of the effective charge is given by the chemical potential of the electrons, i.e., the Fermi level which is usually referenced to the top of the valence band (E_{VBM}) [54,55]. In our work, we focus on the relative stability of two competing phases when vacancies are changed from 0 to +2 instead of the stability of the charged vacancies themselves. We are comparing two specific phases at the same charge state; when comparing the energy difference between them, the term of chemical potential of atoms is canceled. As for the energy of the electrons, considering that the two competing phases have a common energy reference at charge neutrality, it is not proper to set the E_{VBM} of the two phases as reference energy separately. Therefore, we uniquely select the defect levels that have been ignored in previous work as a reference.

In ferroelectric HfO_2 films, it is often observed that oxygen vacancies migrate from the interface to the bulk region during an electric field cycling process [23,25]. The calculated oxygen vacancy diffusion activation energy (E_a) of the M phase and the PO phase are 2.89 and 2.49 eV for $\mathrm{V_O}$, respectively, as shown in Fig. 4(a), consistent with the value of 2.4–3.2 eV reported in previous works [29,30,56]. Such a large diffusion barrier essentially prohibits the migration of $\mathrm{V_O}$. Our calculations show that $\mathrm{V_O^{2+}}$ has a much lower E_a of 0.98 and 0.85 eV

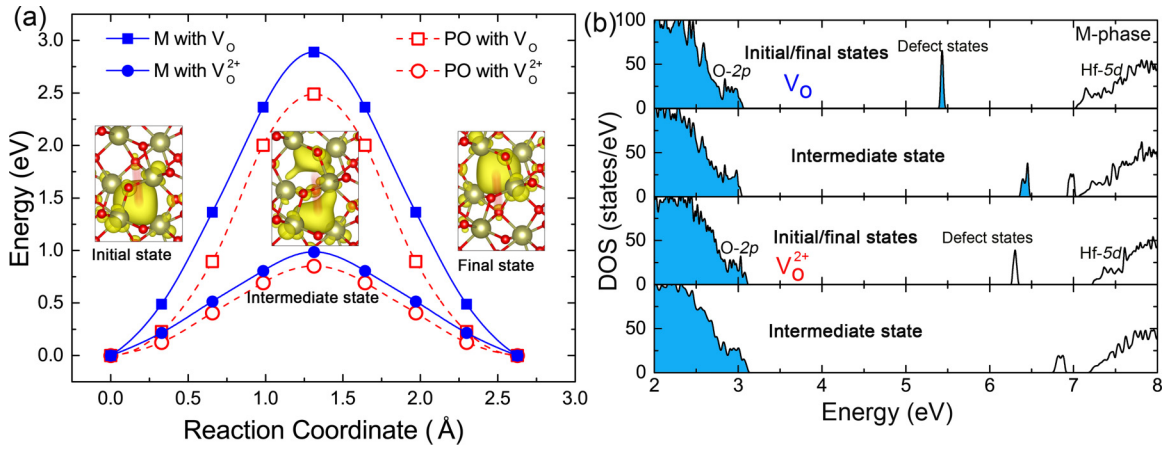

FIG. 4. (a) The energy variation of the V_O and V_O^{2+} during their migrations along the pathways shown in the inset and yellow surface represents the charge density isosurface of the defect state; (b) the corresponding density of states of initial/final and intermediate states with V_O and V_O^{2+} of M-phase HfO_2.

for the M and PO phases respectively, as shown in Fig. 4(a), which indicates that the mobile oxygen vacancy observed in experiments is likely at a charged state such as V_O^{2+}. The diffusion results of E_a are shown to be in agreement with those measured for positively charged oxygen vacancies with an activation energy of 0.52 eV in thin HfO_2 films [24], as well as DFT calculation activation energy barriers of 0.69 eV in the M phase in previous work [29]. Similarly, the reason for the decrease in E_a can be found in the electronic structure. As shown in Fig. 4(b), for the initial configuration with a V_O, the two excess electrons, corresponding to the doubly occupied defect state within the band gap, are strongly localized at the vacancy site. During the oxygen vacancy migration, the two localized electrons hinder the migration of neighboring oxygen atoms. At an intermediate state, the two localized electrons become delocalized and transfer to a defect state with higher energy, resulting in a higher E_a. For V_O^{2+}, the in-gap defect states are unoccupied and there is no effective charge at the vacancy site to oppose the incoming oxygen atom during the diffusion, and the E_a is significantly lower. A similar trend has also been observed in ZrO_2 [57,58] and other oxides [59,60].

In summary, using first-principles DFT calculations, we systematically compared the effects of the V_O^{2+} and V_O on atomic/electronic structures, electric polarization, phase stability, and the activation energy of oxygen vacancy diffusion in HfO_2. As the concentration of V_O^{2+} increases to greater than ∼2%, the ferroelectric PO phase becomes more thermodynamically stable than the M phase, which indicates that V_O^{2+} can help stabilize the ferroelectric phase in HfO_2. We propose a general relationship between the energy in-gap defect levels and relative phase stability in the presence of V_O^{2+} in wide band gap oxides. It is also found that compared to V_O, V_O^{2+} has lower vacancy diffusion activation energy, likely responsible for the observed oxygen vacancy migrations in experiments. These results suggest that compared to the V_O, the theoretically predicted behavior of V_O^{2+} is in better agreement with that observed in experiments. These results may be helpful for the understanding of the origin of ferroelectricity in HfO_2 and pave another way for researching competing structural phases in wide band gap materials.

We are grateful to X. R. Wang for valuable discussion. This work was supported by the National Key R&D Program of China (Grant No. 2017YFA0303602), the Key Research Program of Frontier Sciences of CAS (Grant No. ZDBS-LY-SLH008), the National Nature Science Foundation of China (Grants No. 11774360 and No. 11974365), and the 3315 program of Ningbo. S.L. acknowledges support by Westlake Education Foundation and National Natural Science Foundation of China (12074319). H.L. was supported by Tsinghua-Foshan Innovation Special Fund (TFISF) (2020THFS0132). Calculations were performed at the Supercomputing Center of Ningbo Institute of Materials Technology and Engineering.

[1] T. S. Böscke, J. Müller, D. Bräuhaus, U. Schröder, and U. Böttger, Appl. Phys. Lett. **99**, 102903 (2011).

[2] T. S. Böscke, S. Teichert, D. Bräuhaus, J. Müller, U. Schröder, U. Böttge, and T. Mikolajick, Appl. Phys. Lett. **99**, 112904 (2011).

[3] J. Müller, U. Schröder, T. S. Böscke, I. Müller, U. Böttger, L. Wilde, J. Sundqvist, M. Lemberger, P. Kücher, T. Mikolajick *et al.*, J. Appl. Phys. **110**, 114113 (2011).

[4] S. Mueller, J. Mueller, A. Singh, S. Riedel, J. Sundqvist, U. Schroeder, and T. Mikolajick, Adv. Funct. Mater. **22**, 2412 (2012).

[5] H.-J. Lee, M. Lee, K. Lee, J. Jo, H. Yang, Y. Kim, S. C. Chae, U. Waghmare, and J. H. Lee, Science **369**, 1343 (2020).

[6] S. S. Cheema, D. Kwon, N. Shanker, R. dos Reis, S. L. Hsu, J. Xiao, H. Zhang, R. Wagner, A. Datar, M. R. McCarter *et al.*, Nature (London) **580**, 478 (2020).

[7] J. Müller, T. S. Böscke, U. Schröder, S. Mueller, D. Bräuhaus, U. Böttger, L. Frey, and T. Mikolajick, Nano Lett. **12**, 4318 (2012).

[8] X. Sang, E. D. Grimley, T. Schenk, U. Schroeder, and J. M. LeBeau, Appl. Phys. Lett. **106**, 162905 (2015).

[9] M. H. Park, Y. H. Lee, H. J. Kim, Y. J. Kim, T. Moon, K. D. Kim, J. Müller, A. Kersch, U. Schroeder, T. Mikolajick *et al.*, Adv. Mater. **27**, 1811 (2015).

[10] T. D. Huan, V. Sharma, G. A. Rossetti, and R. Ramprasad, Phys. Rev. B **90**, 064111 (2014).

[11] R. Materlik, C. Künneth, and A. Kersch, J. Appl. Phys. **117**, 134109 (2015).

[12] M. H. Park, T. Schenk, C. M. Fancher, E. D. Grimley, C. Zhou, C. Richter, J. M. LeBeau, J. L. Jones, T. Mikolajick, and U. Schröder, J. Mater. Chem. C **5**, 4677 (2017).

[13] E. D. Grimley, T. Schenk, T. Mikolajick, U. Schroeder, and J. M. LeBeau, Adv. Mater. Interfaces **5**, 1701258 (2018).

[14] C. Künneth, R. Materlik, M. Falkowski, and A. Kersch, ACS Appl. Nano Mater. **1**, 254 (2018).

[15] Y. Zhou, Y. K. Zhang, Q. Yang, J. Jiang, P. Fan, M. Liao, and Y. C. Zhou, Comput. Mater. Sci. **167**, 143 (2019).

[16] R. Batra, T. D. Huan, J. L. Jones, G. Rossetti, and R. Ramprasad, J. Phys. Chem. C **121**, 4139 (2017).

[17] P. Fan, Y. K. Zhang, Q. Yang, J. Jiang, L. M. Jiang, M. Liao, and Y. C. Zhou, J. Phys. Chem. C **123**, 21743 (2019).

[18] M. H. Park, Y. H. Lee, H. J. Kim, T. Schenk, W. Lee, K. D. Kim, F. P. G. Fengler, T. Mikolajick, U. Schroeder, and C. S. Hwang, Nanoscale **9**, 9973 (2017).

[19] Y. Qi, S. Singh, C. Lau, F.-T. Huang, X. Xu, F. J. Walker, C. H. Ahn, S.-W. Cheong, and K. M. Rabe, Phys. Rev. Lett. **125**, 257603 (2020).

[20] S. E. Reyes-Lillo, K. F. Garrity, and K. M. Rabe, Phys. Rev. B **90**, 140103 (2014).

[21] S. Liu and B. M. Hanrahan, Phys. Rev. Mater. **3**, 054404 (2019).

[22] X. Xu, F.-T. Huang, Y. Qi, S. Singh, K. M. Rabe, D. Obeysekera, J. Yang, M.-W. Chu, and S.-W. Cheong, Nat. Mater. **20**, 826 (2021).

[23] M. Pešić, F. P. G. Fengler, L. Larcher, A. Padovani, T. Schenk, E. D. Grimley, X. Sang, J. M. LeBeau, S. Slesazeck, U. Schroeder *et al.*, Adv. Funct. Mater. **26**, 4601 (2016).

[24] S. Zafar, H. Jagannathan, L. F. Edge, and D. Gupta, Appl. Phys. Lett. **98**, 152903 (2011).

[25] E. D. Grimley, T. Schenk, X. Sang, M. Pešić, U. Schroeder, T. Mikolajick, and J. M. LeBeau, Adv. Electron. Mater. **2**, 1600173 (2016).

[26] A. Pal, V. K. Narasimhan, S. Weeks, K. Littau, D. Pramanik, and T. Chiang, Appl. Phys. Lett. **110**, 022903 (2017).

[27] P. Nukala, M. Ahmadi, Y. Wei, S. De Graaf, E. Stylianidis, T. Chakrabortty, S. Matzen, H. W. Zandbergen, A. Björling, and D. Mannix, Science **372**, 630 (2021).

[28] M. Hoffmann, U. Schroeder, T. Schenk, T. Shimizu, H. Funakubo, O. Sakata, D. Pohl, M. Drescher, C. Adelmann, R. Materlik *et al.*, J. Appl. Phys. **118**, 072006 (2015).

[29] N. Capron, P. Broqvist, and A. Pasquarello, Appl. Phys. Lett. **91**, 192905 (2007).

[30] C. Tang, B. Tuttle, and R. Ramprasad, Phys. Rev. B **76**, 073306 (2007).

[31] S. Starschich, S. Menzel, and U. Böttger, Appl. Phys. Lett. **108**, 032903 (2016).

[32] C. Freysoldt, B. Grabowski, T. Hickel, J. Neugebauer, G. Kresse, A. Janotti, and C. G. Van de Walle, Rev. Mod. Phys. **86**, 253 (2014).

[33] S. T. Pantelides, Rev. Mod. Phys. **50**, 797 (1978).

[34] D. M. Ramo, A. Shluger, J. Gavartin, and G. Bersuker, Phys. Rev. Lett. **99**, 155504 (2007).

[35] D. M. Ramo, J. Gavartin, A. Shluger, and G. Bersuker, Phys. Rev. B **75**, 205336 (2007).

[36] S. Fabris, A. T. Paxton, and M. W. Finnis, Acta Mater. **50**, 5171 (2002).

[37] See Supplemental Material at http://link.aps.org/supplemental/10.1103/PhysRevB.104.L180102 for methods, Tables S1–S5, and Figs. S1–S7; also see Refs. [10,11,21,28,38–47].

[38] E. Cockayne, Phys. Rev. B **75**, 094103 (2007).

[39] G. Kresse and J. Furthmüller, Comput. Mater. Sci. **6**, 15 (1996).

[40] J. P. Perdew, A. Ruzsinszky, G. I. Csonka, O. A. Vydrov, G. E. Scuseria, L. A. Constantin, X. Zhou, and K. Burke, Phys. Rev. Lett. **100**, 136406 (2008).

[41] V. V. Afanas'ev, A. Stesmans, F. Chen, X. Shi, and S. A. Campbell, Appl. Phys. Lett. **81**, 1053 (2002).

[42] J. Heyd, G. E. Scuseria, and M. Ernzerhof, J. Chem. Phys. **118**, 8207 (2003).

[43] C. Freysoldt, J. Neugebauer, and C. G. Van de Walle, Phys. Rev. Lett. **102**, 016402 (2009).

[44] J. X. Zheng, G. Ceder, T. Maxisch, W. K. Chim, and W. K. Choi, Phys. Rev. B **75**, 104112 (2007).

[45] S. Clima, D. J. Wouters, C. Adelmann, T. Schenk, U. Schroeder, M. Jurczak, and G. Pourtois, Appl. Phys. Lett. **104**, 092906 (2014).

[46] G. Mills, H. Jónsson, and G. K. Schenter, Surf. Sci. **324**, 305 (1995).

[47] M. D. Glinchuk, A. N. Morozovska, A. Lukowiak, W. Strek, M. V. Silibin, D. V. Karpinsky, Y. Kim, S. V. Kalinin, J. Alloy. Compd. **830**, 153628 (2020).

[48] D. D. Cuong, B. Lee, K. M. Choi, H.-S. Ahn, S. Han, and J. Lee, Phys. Rev. Lett. **98**, 115503 (2007).

[49] A. Alkauskas, P. Broqvist, and A. Pasquarello, Phys. Rev. Lett. **101**, 046405 (2008).

[50] S. Matsuishi, Y. Toda, M. Miyakawa, K. Hayashi, T. Kamiya, M. Hirano, I. Tanaka, and H. Hosono, Science **301**, 626 (2003).

[51] S. Zhang, S.-H. Wei, and A. Zunger, Phys. Rev. B **63**, 075205 (2001).

[52] S. Zhang and J. E. Northrup, Phys. Rev. Lett. **67**, 2339 (1991).

[53] C. G. Van de Walle, D. Laks, G. Neumark, and S. Pantelides, Phys. Rev. B **47**, 9425 (1993).

[54] G. M. Dalpian and S.-H. Wei, Phys. Rev. Lett. **93**, 216401 (2004).

[55] G. M. Dalpian, Y. Yan, and S.-H. Wei, Appl. Phys. Lett. **89**, 011907 (2006).

[56] Y. Dai, Z. Pan, F. Wang, and X. Li, AIP Adv. **6**, 085209 (2016).

[57] A. S. Foster, V. Sulimov, F. L. Gejo, A. Shluger, and R. M. Nieminen, Phys. Rev. B **64**, 224108 (2001).

[58] J. Yang, M. Youssef, and B. Yildiz, Phys. Rev. B **97**, 024114 (2018).

[59] A. Kyrtsos, M. Matsubara, and E. Bellotti, Phys. Rev. B **95**, 245202 (2017).

[60] M. Y. Yang, K. Kamiya, B. Magyari-Köpe, M. Niwa, Y. Nishi, and K. Shiraishi, Appl. Phys. Lett. **103**, 093504 (2013).